

Analysis Note 35: BRAHMS TOF UPDATE

08 July 2001

D. Ouerdane and I.G. Bearden,
Neils Bohr Intitute

1 Introduction

This note presents the latest advances in the Time of Flight (TOF) Calibration software. Results are presented only for the FFS (that is, TOF1), but the software should be applicable for all TOF subsystems. After calibration, we measure a TOF resolution of 105ps, rather better than the 130ps previously obtained. The major improvement from the earlier results is that we now use the channel by channel calibrations for the TDCs, and the effective speed of light (denoted by c_{scint}) is now obtained for each slat. In addition, we now perform a slewing correction for the TOF slats.

2 Software

The calibrations presented here have been obtained using the classes `BrTofCscintCalModule` and `BrTofDeltaDelayCalModule`. Some, but not yet all of the software employed is publically available. All will be public by the end of Week 28.

3 Method: Matching TOF hits to tracks

Meaningful TOF calibrations in the Forward Spectrometer arm require one to first reconstruct tracks to the TOF subsystem under consideration. Having obtained tracks, one knows the track length and can match the track to the appropriate TOF hit. The mathing is accomplished by projecting a track from a tracking chamber to the plane of the TOF subsystem (*e.g.* from T2 to TOF1) and finding the closest TOF hit. We have chosen to first search for the closest hit in X. We define a slat as being *hit* if the slat has a valid time in the TDCs corresponding to the top and bottom tubes, and that the signal in the corresponding ADCs is above threshold. One notes that this immediately removes from consideration any slat for which there is a problem in one of the four (2 TDC, 2 ADC) associated channels (and is perhaps too strict a requirement). The X position of the hit is given by the location of the slat. The Y position can only be obtained after calibrating the effective speed of light in the slat, as well as the offset (that is, we require that the middle of the slat corresponds to $Y=0$).

The following figures illustrate the matching procedure.

Figure 1 shows where in Y global tracks intersect TOF1. Note that this plot has nothing to do with the performance of TOF1; it is only the intersection of the track line with the plane in which TOF1 lies.

The effective speed of light is obtained from the slope of the line describing the difference in the time registered by the top and bottom channels of a give slat versus the Y position on the slat, obtained as described, of the impinging particle. The curves for all slats (before offset calibration) are show in Figure 2

One can, of course, also plot the X distribution of the projected tracks. Of more interest is the difference between the location of the track on TOF1 and the hits according to TOF1. Such plots allow one to assess how correlated the TOF hits are to the projected tracks. Figure 3 exhibits such a plot for TOF1. Here we show the difference between the TOF x postion and the track hit x position for all combinations of valid hit and projected track. The result is a broad background of uncorrelated pairs on top of which is a narrow (one slat width) peak of correlated pairs. Note that Figure 3 shows all pairs. The actual selection is done by finding the hit closest to the projected track. Such a plot can also be produced in Y, and is shown in Figure 4. In this figure the uncorrelated background is assymmetric due to the assymmetric distrubion (in Y, see Figure 1) of projected tracks.

Such a plot can also be produced in Y, and is shown in Figure 4. In this figure the uncorrelated background is assymmetric due to the assymmetric distrubion (in Y, see Figure 1) of projected tracks. Now that we have both ΔX and ΔY , we can find the hit which is the best match to a given track. In this context, “best” means that hit which is closest in X, and for which the magnitude of ΔY is less than $2\sigma_{\Delta Y}$. These hits are now considered part of the track, and we can now, for each track, associate a TOF time to a track length to obtain the velocity of the particle which produced the track.

4 Method: PID

As soon as we have both a calibrated time and a global track, we can begin to asses the extent to which we can do particle identification (PID). The information we possess is: the track momentum and length and the time of flight to the given TOF subsystem (in this case, TOF1). It should be noted that the the track length we use assumes that the particle producing the TOF hit originated at the collision vertex followed a straight trajectory from there to the opening of D1. We also assume that particles fly straight through the magnets, and thus underestimate the path length very slightly (a few millimeters, at the most). We then plot the calculated time for a for a particle with the measured velocity to fly a fixed distance (and thus remove the effect of the moving vertex), and plot this quantity as a function of momentum times charge state (i.e. anti-particles are shown with negative momentum).

If one makes such a plot only matching hits in X, as in Figure 5, one sees clearly a band of particles corresponding (primarily) to pions (although there can certainly be muon and eelectron contamination). In addition, one sees small bands for kaons and anti-protons. There seems to be a wash of background between the various particle types, as well as for longer times. To try to clean this up, we require that track and hit match in Y as well as in X, and the

results are shown in Figure 6 where we see that most of the background with large TOF is now gone. This happens because the requirement that the hit and track match in Y removes, for example, those tracks which point to slats with more than one hit (which will be perfectly well correlated in X, but not at all in time).

In both Figure 5 and Figure 6 attention was drawn to the band of particles on the positive momentum side which would seem to be due to protons. A closer look at these particles reveals that these have TOFs too small to be consistent with protons originating from the collision. It is not yet clear what the source of these particles is, we hypothesize that they may be protons originating from the beam pipe (and thus from $\pi + Be$ reactions) although we have yet to do the work to confirm or deny this hypothesis. At any rate, these tracks which produce these counts do not point back to the collision vertex. We project the FFS tracks back to the X-Y plane of the collision (*i.e.* the X-Y plane at the vertex, as determined by the BB detector), and require that the projected track line within a radius of 5 cm of the assumed reaction vertex (here, we assume that the collision occur at the space point (0,0, BB vertex)). This is shown in Figure 7.

Selecting only tracks which originate from the collision, we again inspect the momentum versus TOF, shown in Figure 8

and we see that the PID has improved. This can also be seen in the mass squared plot in Figure 9, which presents the mass squared distributions for $|p| < 3\text{GeV}/c$, $|p| < 4\text{GeV}/c$, and $|p| < 5\text{GeV}/c$. One notes that the anti-proton peak is clearly resolved at least to $4\text{GeV}/c$, but that valley between the anti-protons and π/K^- peak is somewhat less pronounced when including data up to $5\text{GeV}/c$.

The only major correction to the data which has yet to be taken into account is the slewing correction for the TOF1 slats. This has now been done, using prototype software. The mass squared obtained after slewing correction is shown in Figure 10, which shows that we can separate protons from π, K up to about $5.5\text{ GeV}/c$.

5 Summary

The PID has been improved by including the calibrations for the TDCs (previously, we assumed that all were 25 ps/channel), and c_{scint} calibrations (previously we assumed this was the same for all channels) for each slat. Slewing corrections have also been applied. We find now that we can identify (anti)protons up to $5.5\text{ GeV}/c$, and kaons up to $3\text{ GeV}/c$.

6 To Do

Among the most immediate tasks:

1. Test calibration software in BRAT2.

2. Finish software documentation.
3. Make all software publically available.
4. Produce dN/dy for (anti)protons.
5. Calibrate and analyze 200 GeV data as soon as it becomes available.

7 Finally...

Any questions regarding this document and the results herein should be directed to I.G. Bearden, bearden@nbi.dk. Any and all comments and suggestions are very welcome. I will respond to such comments via the listserver brahms-1@bnl.gov so that all may enjoy the wisdom of my reply. This analysis was done using BRAT-1-16-3. We are presently testing the software employed with BRAT2.

All of the credit for the analysis should go to D. Ouerdane, mistakes and mistatements in the text are due to I. G. Bearden.

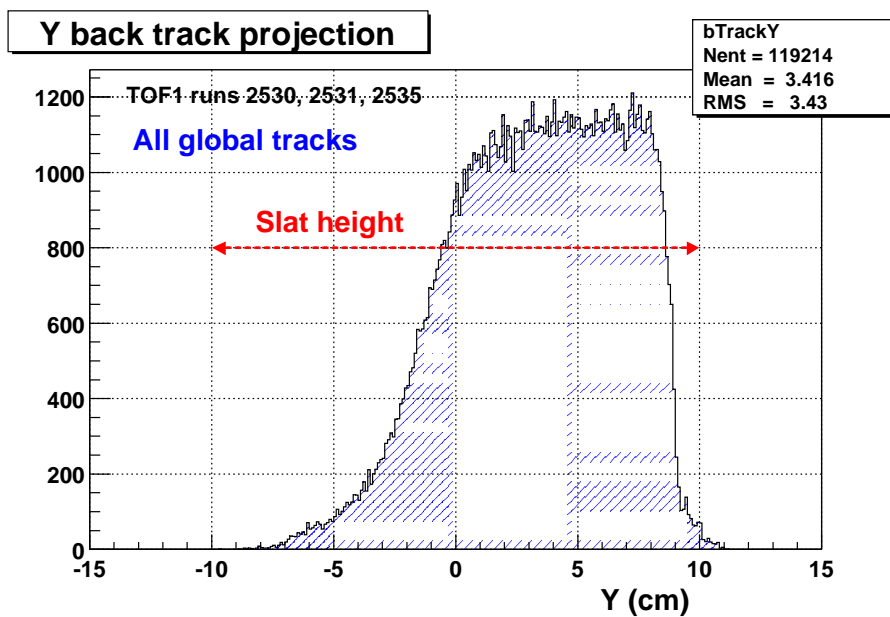
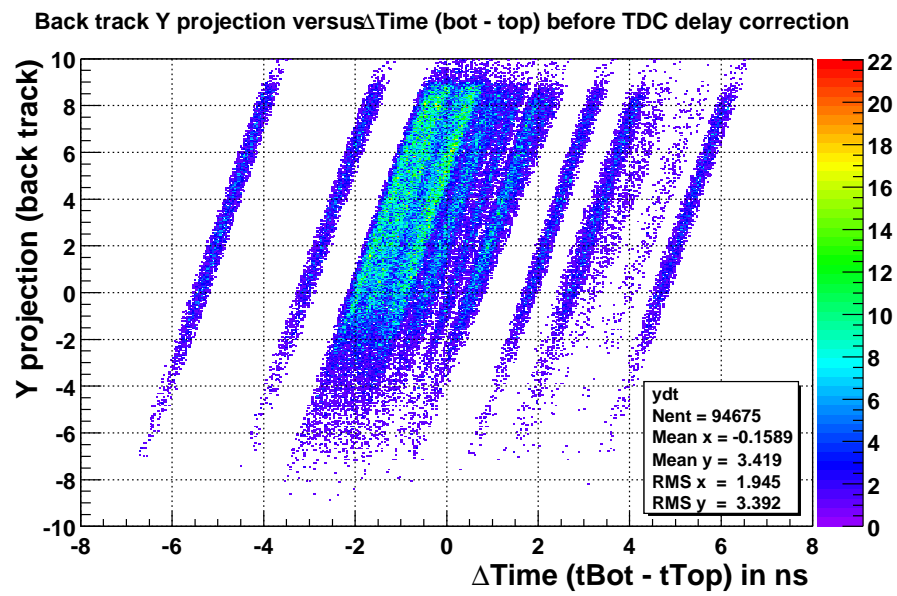
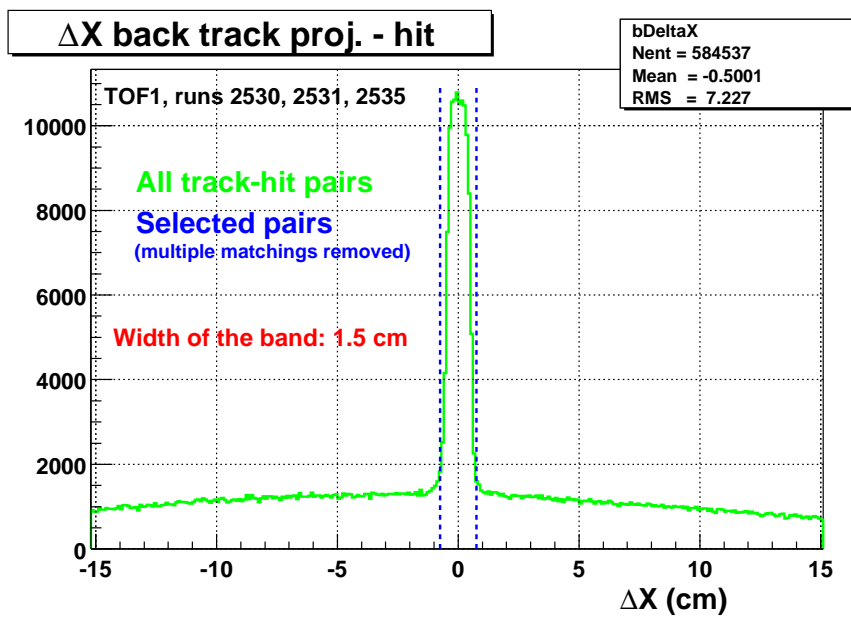


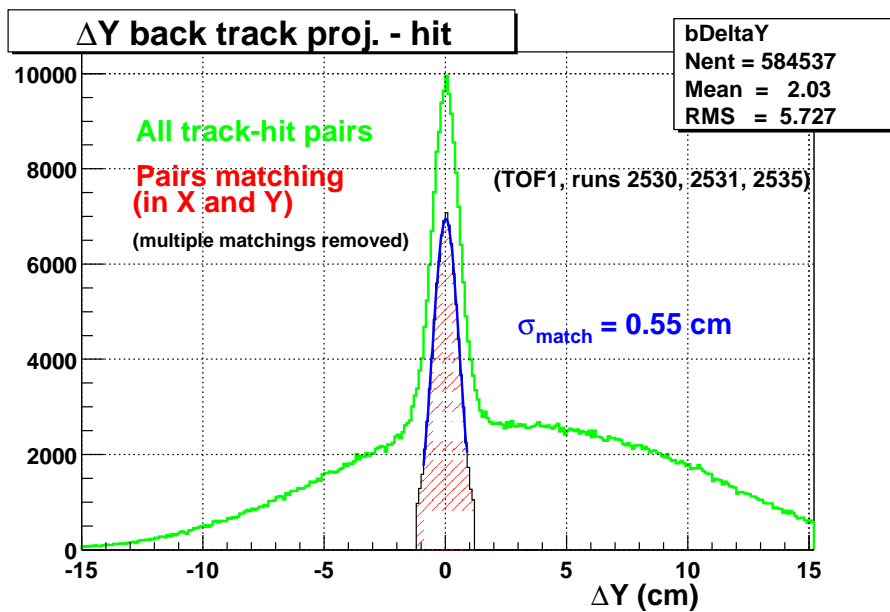
Figure 1: Y distribution of global tracks projected onto TOF1. One notes that there are few tracks with $y < 0$, this is due to inefficiencies in T2 presumably associated with the gas flow features of that detector.



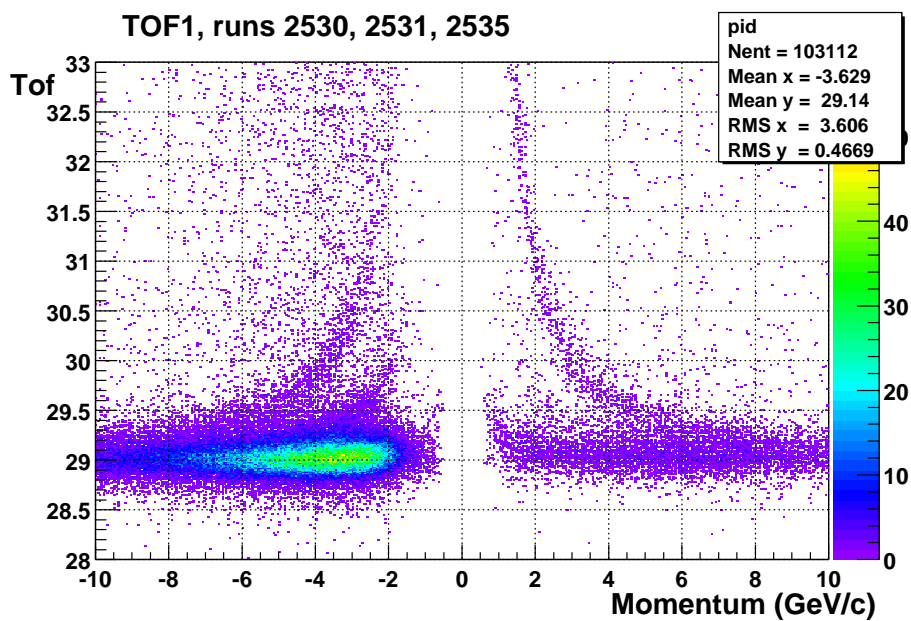
Figur 2: Y projection of track versus time difference (bottom - top) in the same slat. This is for all slats, prior to offset calibration.



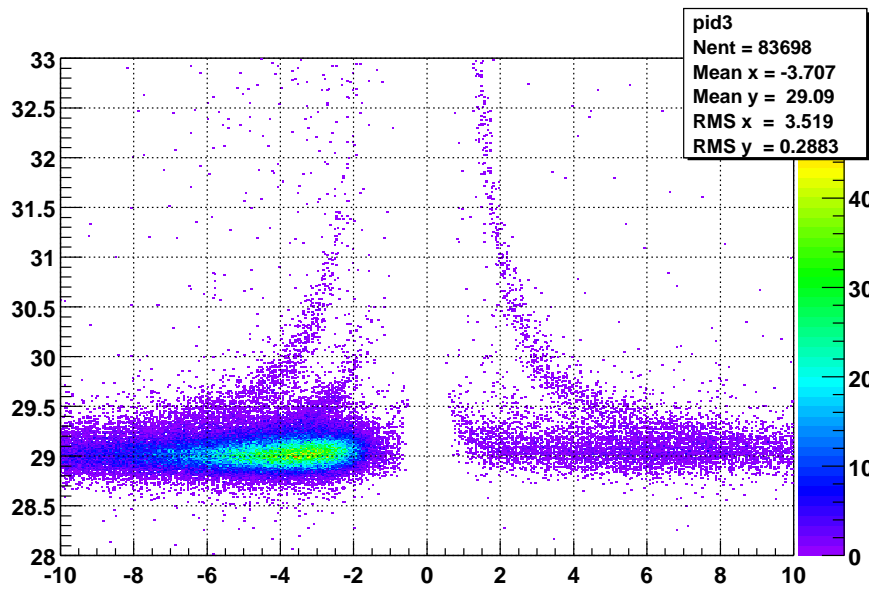
Figur 3: Difference in TOF hit and projected track X position. The background is due to the uncorrelated tracks and hits, while the peak (which is approximately one slat wide, as it should be) shows that there tracks and hits which are correlated.



Figur 4: Difference in TOF hit and projected track Y position. The background is assymmetric due to T2 inefficiency. The red filled histogram shows those pairs for which the hit is closest in both X and Y to the projected track, and for which ΔX is less than 0.75 slat widths. The width of the narrow gaussian is related to the time resolution, but will raise questions in the mind of the clever reader.



Figur 5: Calculated TOF versus momentum for runs 2530, 2531, 2535. Note that the magnets are set to select negatively charged particles. The TOF hits are matched in X position only, and no clean up cuts have been applied to the tracks. The proton like band is due to background and is discussed in the text.



Figur 6: Calculated TOF versus momentum for runs 2530, 2531, 2535. Note that the magnets are set to select negatively charged particles. The TOF hits are matched in X and in Y, but no clean up cuts have been applied to the tracks. Now the K^- and anti-proton signals are quite clear. The (positive) proton like band is due to background and is discussed in the text.

Track projection on BB vertex plane

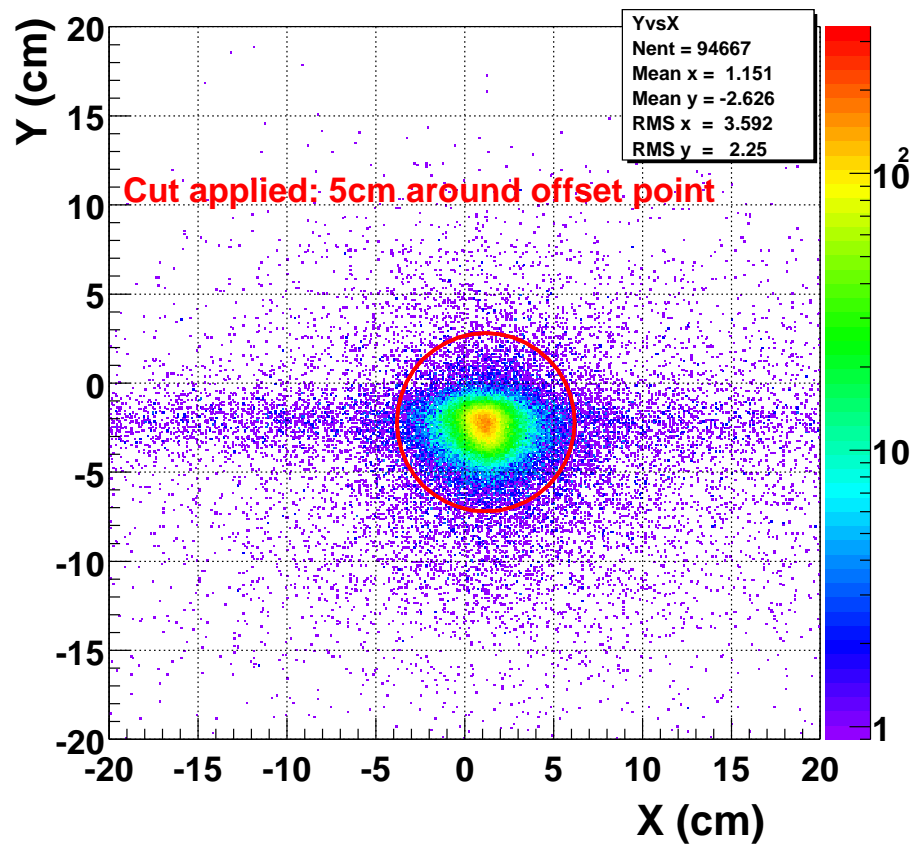
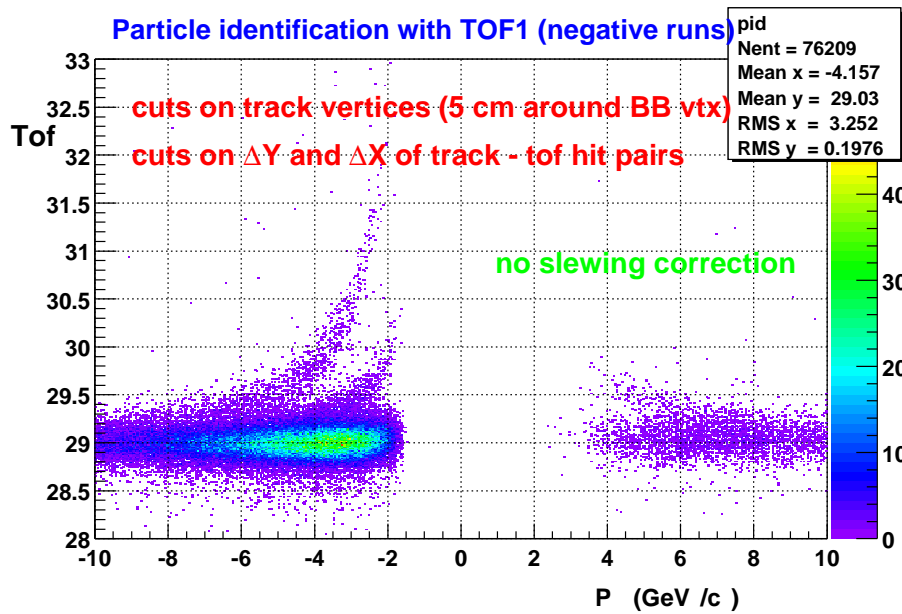
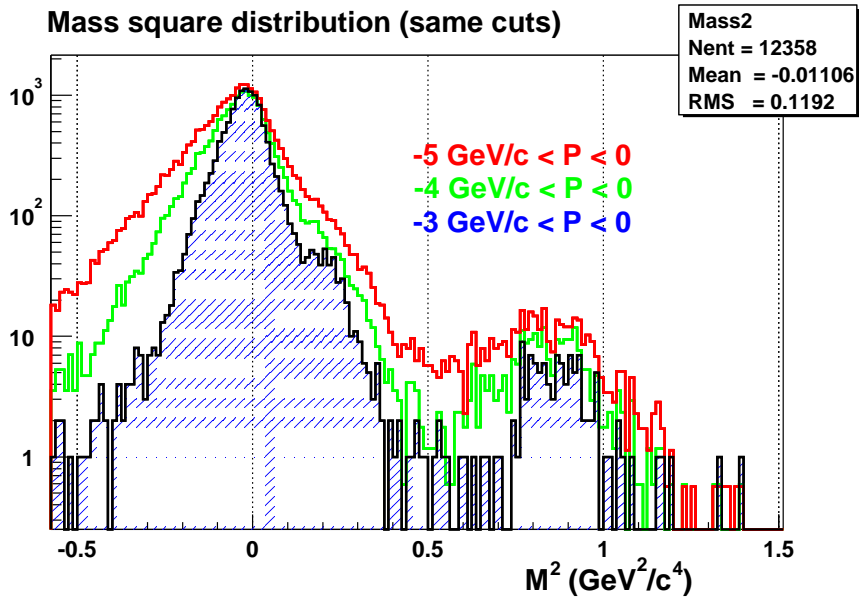


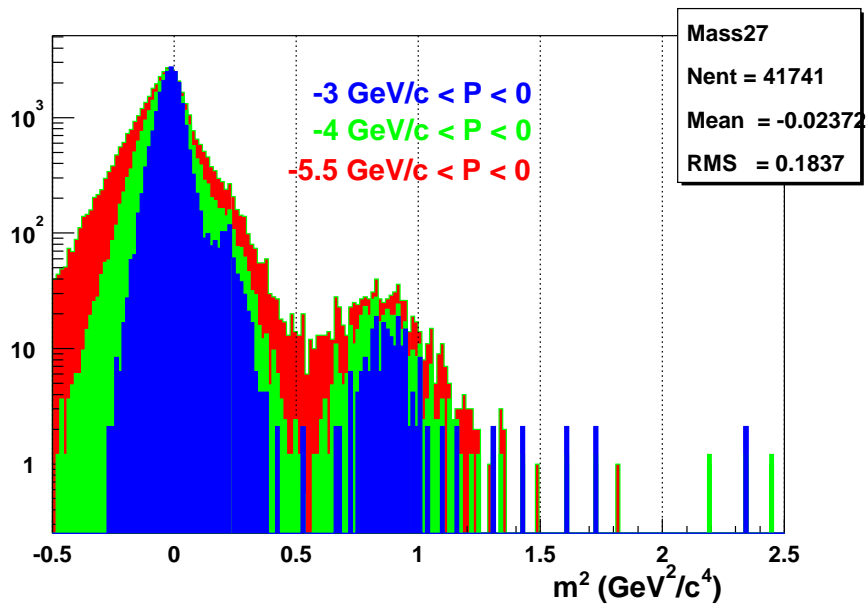
Figure 7: Projection of the FFS track back to the X-Y plane of the collision. We select only those events which lie within 5cm of the reaction point.



Figur 8: Calculated TOF versus momentum for runs 2530, 2531, 2535. Note that the magnets are set to select negatively charged particles. The TOF hits are matched in X and in Y, and the tracks are required to point back to the interaction vertex. Now the K^- and anti-proton signals are obvious. The number of counts with large TOF times has been reduced, as has the background between the K^- and anti-proton bands. The (positive) proton like band has been removed by the vertex cut.



Figur 9: Mass squared for $|p| < 3\text{GeV}/c$ (blue filled), $|p| < 4\text{GeV}/c$ (green), and $|p| < 5\text{GeV}/c$ (red).



Figur 10: Mass squared for $|p| < 3\text{GeV}/c$ (blue filled), $|p| < 4\text{GeV}/c$ (green filled), and $|p| < 5.5\text{GeV}/c$ (red filled) after slewing corrections.